

## THE MANY SCALES IN THE UNIVERSE

# The Many Scales in the Universe

JENAM 2004 Astrophysics Reviews

*Edited by*

**J.C. DEL TORO INIESTA**

*Instituto de Astrofísica de Andalucía, CSIC, Spain*

**E.J. ALFARO**

*Instituto de Astrofísica de Andalucía, CSIC, Spain*

**J.G. GORGAS**

*Universidad Complutense de Madrid, Spain*

**E. SALVADOR-SOLÉ**

*Universitat de Barcelona, Spain*

and

**H. BUTCHER**

*ASTRON, Dwingeloo, The Netherlands*

 Springer

A C.I.P. Catalogue record for this book is available from the Library of Congress.

ISBN-10 1-4020-4351-1 (HB)  
ISBN-13 978-1-4020-4351-2 (HB)  
ISBN-10 1-4020-4526-3 (e-book)  
ISBN-13 978-1-4020-4526-4 (e-book)

---

Published by Springer,  
P.O. Box 17, 3300 AA Dordrecht, The Netherlands.

*www.springer.com*

*Printed on acid-free paper*

All Rights Reserved

© 2006 Springer

No part of this work may be reproduced, stored in a retrieval system, or transmitted in any form or by any means, electronic, mechanical, photocopying, microfilming, recording or otherwise, without written permission from the Publisher, with the exception of any material supplied specifically for the purpose of being entered and executed on a computer system, for exclusive use by the purchaser of the work.

Printed in the Netherlands.

# Contents

Preface	xi
Committees	xv
The Cosmic Microwave Background Anisotropies: Open Problems	1
<i>Enrique Martínez-González and Patricio Vielva</i>	
1 Introduction	2
2 CMB temperature anisotropies	4
3 Polarization	8
4 Cosmological parameters	9
5 Cosmological constraints	11
6 Open problems	17
Acknowledgments	20
References	21
The Gravitational Lensing Effect in Cosmology	25
<i>Genevieve Soucail</i>	
1 Basics of gravitational lensing	25
2 Strong lensing in clusters of galaxies	27
3 From weak lensing to masses	30
4 The cosmic shear or lensing by large scale structures	32
5 Conclusions	33
References	34
The PLANCK Mission	35
<i>J.A. Tauber</i>	
1 Introduction	35
2 Payload	36
3 Programmatic aspects	36
4 Scientific performance	38
5 Mission profile	40
6 Operations and data processing	42
Acknowledgments	42
References	43



Surveys of Extragalactic Sources with PLANCK	45
<i>G. De Zotti, C. Burigana, M. Negrello, S. Tinti, R. Ricci, L. Silva, J. González-Nuevo and L. Toffolatti</i>	
1    Introduction	46
2    Power spectra of foreground emissions	47
3    30 GHz counts	48
4    350 GHz counts	51
5    Conclusions	53
Acknowledgments	53
References	53
 New Physics in Clusters of Galaxies	 55
<i>M. Douspis</i>	
1    Introduction	55
2    The concordance model	56
3    Dark matter	60
4    The amplitude of fluctuations	61
5    Summary	67
Acknowledgments	68
References	68
 Emission Line Galaxies in Clusters	 71
<i>Bianca M. Poggianti</i>	
1    Introduction	71
2    High redshift	72
3    Physical processes	76
4    Low redshift	77
5    Trends with galaxy mass and downsizing effect	80
6    Conclusions and speculations	80
Acknowledgments	83
References	84
 Active Galactic Nuclei and Surveys: the View from the New X-ray Observatories	 87
<i>X. Barcons</i>	
1    Introduction	87
2    The inner disk: Fe line diagnostics	89
3    The circumnuclear environment	92
4    Challenges to the unified AGN model	93
5    X-ray surveys, obscured accretion and the X-ray background	94
6    Outlook	96
Acknowledgments	96
References	97
 Star-Forming Complexes in Galaxies	 99
<i>Bruce G. Elmegreen</i>	
1    Introduction to star complexes	99

<i>Contents</i>	vii
2 Formation of star complexes	101
3 Characteristic size versus scale-free?	103
4 Theory of the star formation rate	104
5 Conclusions	108
Acknowledgments	109
References	109
Star Formation and Infrared Emission in Galaxies	111
<i>Nikolaos D. Kylafis and Angelos Misiriotis</i>	
1 Introduction	111
2 Model for late-type spiral galaxies	112
3 Correlation between star formation and infrared emission	115
4 Other star formation diagnostics	117
5 Instead of a summary	118
References	119
Evolution of the Milky Way Disk	121
<i>B. Nordström and J. Andersen</i>	
1 Introduction	121
2 Stellar sample and observational data	122
3 Derived astrophysical parameters	124
4 The key diagnostic relations	126
5 Discussion	128
6 Summary	129
Acknowledgments	129
References	130
Massive Stars in the Galactic Center	131
<i>F. Najarro</i>	
1 Introduction	131
2 Improved observations and models	133
3 The quintuplet cluster	135
4 The arches cluster	138
Acknowledgments	143
References	143
The Mass Spectrum of X-Ray Binaries	145
<i>Jorge Casares</i>	
1 Introduction	145
2 Establishing black holes	146
3 Mass determination in persistent LMXBs	151
4 Conclusions	153
Acknowledgments	153
References	154

Massive Stars in Starbursts	155
<i>Alan Pedlar</i>	
1    Introduction	155
2    Estimating starformation rates in messier 82	156
3    Indicators of massive stars	156
4    The age of the supernova remnants in M82	160
5    Summary	163
Acknowledgments	163
References	164
The Hot Content of Planetary Nebulae	165
<i>Martín A. Guerrero, You-Hua Chu and Robert A. Gruendl</i>	
1    Sources of X-ray emission from planetary nebulae	165
2    X-Ray observations of PNe	167
3    The conduction layers in PNe	172
4    Summary	172
References	174
The Hidden Life of Massive Stars	175
<i>A. Lenorzer, A. Bik, M.R. Mokiem, A. de Koter, L. Kaper and L.B.F.M. Waters</i>	
1    Introduction	176
2    Search for young massive stars	176
3    Stellar parameters from near-infrared spectra	177
4    Geometry of the circumstellar material	180
5    Case study: NGC2024/IRS2	182
References	184
What can we learn about the Sun from observations in the near ultraviolet?	187
<i>Achim Gandorfer</i>	
1    Introduction: magnetometry of the solar photosphere	187
2    Scattering polarization and the hanle effect in the near UV	189
3    Solar magnetometry at high spatial resolution: The role of SUNRISE	193
4    Summary	195
References	195
Our Magnetic Sun	197
<i>E.R. Priest</i>	
1    Introduction	197
2    Overall structure of the Sun	199
3    The corona	201
4    MHD and reconnection	202
5    The solar and heliospheric observatory (SOHO)	204
6    Conclusions	208
Acknowledgments	209
References	209

<i>Contents</i>	ix
Moist Convective Storms in the Atmospheres of Jupiter and Saturn	211
<i>Ricardo Hueso and Agustín Sánchez-Lavega</i>	
1 Introduction	211
2 Observations of convective storms in jupiter and saturn	213
3 Modelling moist convective storms	214
4 Storm locations and wind relation	216
5 Conclusions	219
Acknowledgments	219
References	219
Exploring the Solar System beyond Neptune	221
<i>Jose L. Ortiz and Pablo Santos-Sanz</i>	
1 Introduction	221
2 Current knowledge	223
References	232
Planet Detection with Large Telescopes and Interferometry	235
<i>Andreas Quirrenbach</i>	
1 Introduction and general goals	235
2 Coronagraphy with large telescopes	236
3 Extrasolar planets with the VLTI	239
4 The space interferometry mission	244
5 Darwin and the terrestrial planet finder	245
6 Conclusions	249
References	249
AVO First Science	253
<i>Mark G. Allen, Paolo Padovani, Piero Rosati and Nicholas A. Walton</i>	
1 Introduction	253
2 Astrophysical virtual observatory	254
3 Finding type 2 AGN in the goods fields	255
4 Next AVO science developments	259
5 Summary	259
References	260
Euro50: A European 50 M Adaptive Optics Extremely Large Telescope	261
<i>Arne Ardeberg and Torben Andersen</i>	
1 Introduction	261
2 From a Swedish to a European project	262
3 A European ELT – Why?	263
4 A European ELT - How	276
References	289
Author Index	295

## Preface

This book gathers the invited conferences presented at the Thirteenth Joint European and National Astronomical Meeting (JENAM) organized by the European Astronomical Society (EAS) and the Spanish Astronomical Society (Sociedad Española de Astronomía, SEA) and hosted by the Instituto de Astrofísica de Andalucía (IAA - CSIC). The event, held from September 13 to 17, 2004 in Granada, was at the same time the Sixth Scientific Meeting of the SEA. The proceedings of such national meetings are traditionally collected in a series of books generically entitled *Highlights of Spanish Astrophysics*, which will be momentarily interrupted in this occasion as the contributions of the Spanish astronomers to the meeting share the present publication with those of their colleagues from other European countries or, to be more exact, from countries all over the world. The meeting brought together, indeed, more than 450 participants from 30 different countries, making it one of the most successful JENAMs ever celebrated. This success was undoubtedly due to the fact that, as readily seen from the titles of the parallel sessions, the scientific scope of this JENAM reached, for the first time, all fields of astronomy and astrophysics. In fact, there was still another parallel session opened to teachers and professionals of popularisation in astronomy whose proceedings are published elsewhere.

As members of the SOC we were aware about the risk that, in willing to cover all fields of astronomy, no particular topic would be treated duly in depth, which might make the meeting loose interest for potential attendants. For this reason, a dozen of renowned specialists in different fields were invited to review central aspects in the different domains of astrophysics. We want to thank here all of them for the superb *mise á jour* they offered to the audience. These main talks constitute the main body –the printed part– of the present book, becoming in this way an excellent tool for astronomers to have a general up-to-date look on the most exiting items of current astronomical research. The papers are organized per sessions, per scales of the Universe indeed, according to the structure of the meeting; the last session is devoted to instrumentation. It would certainly be a pity not to preserve at the same time the remaining 150 short oral contributions and 324 posters presented at the meeting with interest-

ing results on a variety of specific items. For this reason, attached to the book is a CD including all these contributions in full format. We hope they will be very useful for astronomers working on the corresponding domains.

The Editors  
Granada, July 2005



<http://www.kaa.es/jenam2004/>

# The many scales in the Universe

- Roads to cosmology
- The life of galaxies
- Your favourite stars and their environments
- The Sun and planetary systems
- Real and virtual instruments
- Teaching and communicating astronomy

GRANADA

Joint European and National Astronomical Meeting  
13-17 September, 2004



## **Committees**

### **Honour Committee**

**H.R.H. Felipe de Borbón y Grecia**

Prince of Asturias

**H.E. M<sup>a</sup> Jesús Sansegundo**

Minister of Education and Science

**H.E. Manuel Chaves González**

President of the Autonomous Region of Andalusia

**H.E. Cándida Martínez López**

Counsellor of Education and Science of the Autonomous Region of Andalusia

**H.E. Francisco Vallejo Serrano**

Counsellor of Innovation, Science, and Business of the Autonomous Region of Andalusia

**H.E. Antonio Martínez Caler**

President of the Province of Granada Government

**H.E. José Torres Hurtado**

Mayor of Granada

**H.E. Carlos Martínez Alonso**

President of the National Council for Scientific Research

**H.E. David Aguilar Peña**

President of the University of Granada



**Scientific Organizing Committee**

E.J. Alfaro (Granada, executive co-ordinator)  
G. Bernabéu (Alicante)  
H. Butcher (Dwingeloo, co-chair)  
M. Castellanos (Madrid)  
R. Domínguez–Tenreiro (Madrid)  
F. Figueras (Barcelona)  
M.A. Gómez-Flechoso (Madrid)  
J. Gorgas (Madrid)  
B. Gustaffson (Upsala)  
A. Herrero Davó (La Laguna)  
V. Martínez (Valencia)  
V. Martínez Pillet (La Laguna)  
P. Papaderos (Göttingen)  
J.M. Rodríguez–Espinosa (La Laguna)  
E. Salvador–Solé (Barcelona, co-chair)  
A. Sánchez–Lavega (Bilbao)  
J. Silk (Oxford)  
M. Stavinschi (Bucharest)  
N. Thomas (Bern)  
J.C. del Toro Iniesta (Granada)

**Convenors of the Parallel Sessions****Roads to Cosmology**

R. Domínguez Tenreiro (Madrid)  
E. Gaztañaga (Barcelona)  
J. Silk (Oxford)

**The Life of Galaxies**

J.M. Vílchez (Granada)  
F. Figueras (Barcelona)  
R. Bender (Munich)

**Your Favourite Stars and their Environments**

A. Herrero (La Laguna)  
A. Alberdi (Granada)  
B. Gustaffson (Uppsala)

**The Sun and Planetary Systems**

V. Martínez–Pillet (La Laguna)

A. Sánchez–Lavega (Bilbao)  
N. Thomas (Bern)

**Real and Virtual Instruments**

J.M. Rodríguez–Espinosa (La Laguna)  
A.I. Gómez de Castro (Madrid)  
M. Dennefeld (Paris)

**Teaching and Communicating Astronomy**

V. Martínez (Valencia)  
G. Bernabéu (Alicante)  
M. Stavinschi (Bucharest)

**Local Organizing Committee**

Antxon Alberdi  
Emilio J. Alfaro  
Begoña Ascaso  
Daniel Cabrera  
Benigno Cantero  
Ricardo Casas  
Antonio J. Delgado  
Daniel Espada  
Omaira González–Martín  
Carolina Kehrig  
Lucas Lara  
Silbia López de Lacalle  
M. Ángeles Martínez–Carballo  
David Orozco  
Mayra Osorio  
Daniel Reverte  
José Ruedas  
Jose Carlos del Toro Iniesta (Chair)  
José Sabater  
M. Carmen Sánchez–Gil  
M. Jesús Vidal

# THE COSMIC MICROWAVE BACKGROUND ANISOTROPIES: OPEN PROBLEMS

Enrique Martínez-González and Patricio Vielva  
*Instituto de Física de Cantabria, CSIC-Universidad de Cantabria*  
martinez@ifca.unican.es, vielva@ifca.unican.es

**Abstract** We present a review of some interesting theoretical and observational aspects of the Cosmic Microwave Background anisotropies. The standard inflationary model presents a simple scenario within which the homogeneity, isotropy and flatness of the universe appear as natural outcomes and, in addition, fluctuations in the energy density are originated during the inflationary phase. These seminal density fluctuations give rise to fluctuations in the temperature of the Cosmic Microwave Background (CMB) at the decoupling surface. Afterward, the CMB photons propagate almost freely, with slight gravitational interactions with the evolving gravitational field present in the large scale structure (LSS) of the matter distribution and a low scattering rate with free electrons after the universe becomes reionized by the first stars and QSOs. These secondary effects slightly change the shape of the intensity and polarization angular power spectra of the radiation, the so called  $C_\ell$ . The  $C_\ell$  contain very valuable information on the parameters characterizing the background model of the universe and those parametrising the power spectra of both matter density perturbations and gravitational waves. The extraction of this richness of information from the  $C_\ell$  is complicated by the superposition of the radiation coming from other Galactic and extragalactic emissions at microwave frequencies. In spite of this, in the last few years data from sensitive experiments have allowed a good determination of the shape of the  $C_\ell$ , providing for the first time a model of the universe very close to spatially flat. In particular the WMAP first year data, together with other CMB data at higher resolution and other cosmological data sets, have made possible to determine the cosmological parameters with a precision of a few percent. The most striking aspect of the derived model of the universe is the unknown nature of most of its energy contents. This and other open problems in cosmology represent exciting challenges for the CMB community. The future ESA Planck mission will undoubtedly shed some light on these remaining questions.

**Keywords:** Cosmic Microwave Background, Data Analysis, Cosmological Parameters

## 1. Introduction

In recent years there has been an explosion of cosmological data allowing a strong progress in the characterization of the cosmological model of the universe. In particular, recent data of the temperature of the Cosmic Microwave Background (CMB) have played a crucial role in the determination of the cosmological parameters. Many experiments aimed to map the temperature of the CMB have been and are being carried out, and many others are now being planned to extend present capabilities in resolution and sensitivity. From the cosmological data already collected we know that the spatial geometry of the universe is close to Euclidean, with most of the energy density in the form of the so called "dark energy (DE)" (with an equation of state close to a cosmological constant) and most of the matter density in the form of the so called "cold dark matter (CDM)" (weakly interactive matter with negligible velocity). About the primeval density perturbations we know that they were close to the adiabatic type (constant ratio of the matter number density to photon density for each matter component) and Gaussianly distributed with a nearly scale-invariant power spectrum (i.e. the gravitational potential fluctuations are the same at all scales). The generic predictions of inflation—a very brief episode of drastic expansion in the very early history of the universe close to the Planck time—are consistent with the characteristics of the model of the universe and of the primeval density fluctuations just mentioned, the so called "concordance model". Thus, inflation provides us with a plausible scenario within which we can understand the horizon and flatness problems (i.e. why causally disconnected regions appear statistically similar in the CMB sky and why the density of the universe is so close to the critical one) and also the origin of the density perturbations. Although a physical model of inflation is still lacking, however, it provides us with a phenomenological scenario within which we can conceptually understand some fundamental problems related to the origin of the "special" properties of the universe—i.e. its homogeneity and critical density—and its large scale structure (LSS) matter distribution which otherwise will have to rely on ad hoc initial conditions. In the past decade two of the experiments on-board of the NASA COBE satellite, FIRAS and DMR, established unambiguously the black-body electromagnetic spectrum of this radiation (Mather et al. 1994, 1999) and the level and approximate scale-invariant shape of the spectrum of density fluctuations (Smoot et al. 1992). The former data rebated some previous results which indicated possible distortions from the black-body spectrum, establishing the thermal origin of the CMB with a high precision. The latter confirmed the gravitational instability theory for the formation of the LSS and determined an initial spectrum of fluctuations characterized by density fluctuations with approximately equal amplitude when entering the horizon. These fundamental results set the basis for the

later developments in our understanding of the universe and opened the era of precision cosmology. At the end of the decade several experiments determined that the universe is close to spatially flat (BOOMERANG, De Bernardis et al. 2000; MAXIMA, Hanany et al. 2000). More recently the NASA WMAP satellite (Bennett et al. 2003) nicely confirmed this result and, together with other higher resolution CMB experiments as well as the galaxy survey 2dFGRS (Percival et al. 2001), determined the cosmological parameters with a few percent errors. The combination of different cosmological data sets not only helps to improve the precision of the cosmological parameters but, what is more important, shows the compatibility of the different data sets in the context of the concordance model. The most important features of this model is the distribution of the energy content of the universe with about 70% of dark energy, 25% of cold dark matter (CDM) and only 5% of baryons. The detection of the polarization fluctuations by DASI (Kovac et al. 2002) and the later determination of the temperature-polarization angular cross-power spectrum by WMAP (Kogut et al. 2003) has strongly confirmed the concordance model. Very recently, there have been several works finding evidences of positive cross-correlations between the CMB temperature map and the LSS distribution of galaxies (see e.g. Boughn and Crittenden 2004). These results represent an independent piece of evidence of the existence and dominance of dark energy in the recent history of the evolution of the universe (assuming that the universe is close to flat). Although the concordance  $\Lambda$ CDM model represents a good fit to the CMB data as well as to other cosmological data sets —namely LSS galaxy surveys, primordial Big-Bang nucleosynthesis, measurements of the Hubble constant, SN Ia magnitude-redshift diagram— there are however some problems related to the observations and also to their interpretation.

The aim of this paper is to review some of the most relevant theoretical and observational results on the CMB field and to point out some open problems associated to them. For more detailed discussions the reader is referred to the many good reviews written in the literature, some of them more oriented to the theory (e.g. Hu and Dodelson 2002, Challinor 2004, 2005, Cabella and Kamionkowski 2004) and others to the experiments (e.g. Barreiro 2000, Bersanelli, Maino and Mennella 2002, Mennella et al. 2004).

The rest of this review is as follows. In Section 2 we describe the main properties of the CMB temperature anisotropies and the physical effects that originate them. In Section 3 the most relevant properties of the CMB polarization anisotropies are considered. The cosmological parameters are defined in Section 4 and their values determined from recent CMB data and in combination with other cosmological data sets are presented in Section 5. Finally, open problems in the CMB field are discussed in Section 6.

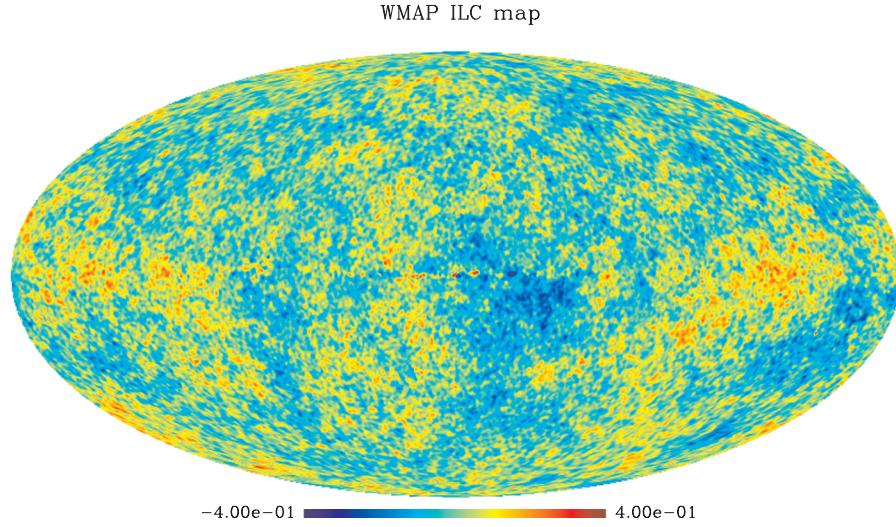


Figure 1. The CMB as seen by WMAP (data obtained from the LAMBDA wave page of NASA).

## 2. CMB temperature anisotropies

### Description

The anisotropies of the CMB—the fluctuations in the intensity of this radiation as a function of the direction in the sky—are interpreted as a realization of a random field on the sphere. Behind this interpretation is the idea that we aim to understand and possibly explain the anisotropies in a statistical manner. Because of the blackbody spectrum of the CMB, the anisotropies in the intensity are generally given as temperature ones. Since the temperature fluctuations are a function of the spherical coordinates it is convenient to expand them in spherical harmonics,

$$\frac{\Delta T}{T}(\vec{n}) = \sum_{\ell, m} a_{\ell m} Y_{\ell m}(\vec{n}), \quad (1)$$

where  $a_{\ell m}$  are the spherical harmonic coefficients. A very important quantity is the CMB anisotropy angular power spectrum,  $C_\ell$ , the second order moment of the  $a_{\ell m}$  defined as

$$\langle a_{\ell m} a_{\ell' m'}^* \rangle = C_\ell \delta_{\ell \ell'} \delta_{m m'}. \quad (2)$$

The null correlation of the harmonic coefficients for different  $\ell$  or  $m$  is due to the homogeneity and isotropy of the universe —i.e. the Cosmological Principle assumed as a fundamental pillar in cosmology and consistent with all of our observations up to date. Here it is important to notice, however, that the previous equation does not hold if the universe possesses a nontrivial topology. An important property of the  $C_\ell$  is that if the anisotropies are Gaussian —as predicted by Inflation— then all the statistical information is contained in it (reported deviations from Gaussianity will be discussed in section 6). The correlation function of the temperature fluctuations,  $C(\theta) \equiv \langle \Delta T/T(\vec{n}_1)\Delta T/T(\vec{n}_2) \rangle$  with  $\vec{n}_1\vec{n}_2 = \cos(\theta)$ , is related to the  $C_\ell$  through the Legendre transform

$$C(\theta) = \sum_{\ell} \frac{2\ell + 1}{4\pi} C_\ell P_\ell(\cos \theta). \quad (3)$$

The isotropy of the field is now reflected in the independence of the correlation from the direction. Although the two quantities  $C(\theta)$  and  $C_\ell$  contain the same information, however the null correlation of the  $C_{\ell_s}$  for different values of  $\ell$  makes the latter quantity preferable for cosmological studies. The quantity which is usually displayed is  $\ell(\ell + 1)C_\ell/2\pi$ , i.e. the power per logarithmic interval in  $\ell$  for large  $\ell$ . Since the  $\ell = 1$  moment is dominated by our motion only moments with  $\ell \geq 2$  are considered.

There is a fundamental limitation in the accuracy with which the angular power spectrum  $C_\ell$  can be determined due to the fact that we can only observe one last-scattering surface —the error associated to it is called “cosmic variance”. Since there are  $2\ell + 1$   $a_{\ell m}$  coefficients for a given  $\ell$  then for Gaussian temperature fluctuations the cosmic variance is easily calculated (from the dispersion of a chi-squared distribution with  $2\ell + 1$  degrees of freedom)

$$\Delta C_\ell = \frac{1}{\sqrt{\ell + 0.5}} C_\ell. \quad (4)$$

There are other sources of error which should be added to the cosmic variance. One is the fraction of the sky  $f_{sky}$  covered by an experiment, which increases the error by a factor  $f_{sky}^{-1/2}$  (Scott et al. 1994). Another one is the sensitivity of the experiment whose noise power spectrum adds to the  $C_\ell$  of the cosmic signal in equation 4. Finally, there is a source of error coming from the process to separate the cosmic signal from the other foregrounds, namely Galactic emissions<sup>1</sup> (synchrotron, free-free and thermal dust), extragalactic sources, galaxy clusters and the lensing effect from the LSS. This is usually a complex task to perform which requires multifrequency observations and whose error is difficult to estimate a priori. Estimate of the errors assuming different situations

---

<sup>1</sup>See e.g. Watson et al. (2005) for evidence of possible anomalous Galactic emission



and methodology can be found in, e.g., Hobson et al. (1998), Tegmark et al. (2000), Bouchet and Gispert (1999), Vielva et al. (2001), Maino et al. (2002), Herranz et al. (2002), Martínez-González et al. (2003), Delabrouille et al. (2003).

In figure 1 the map of temperature anisotropies as measured by WMAP is shown (Bennett et al. 2003). Although a large effort has been made to eliminate all foreground contributions however some residuals from Galactic foregrounds can still be seen in the central horizontal band of this map. In order to avoid the introduction of this contamination in the data analysis a mask covering that and other regions of the map is usually applied.

## Physics

The CMB anisotropies are usually divided in primary and secondary, depending if they are produced before or after the last-scattering surface. The primary anisotropies are the most interesting ones to study the cosmological parameters characterising the universe as well as its basic matter and energy constituents. The secondary ones are produced by scattering of the CMB photons from ionized matter —either generated after the reionization of the universe or present as hot gas in the central regions of galaxy clusters and whose interaction with the CMB photons is known as the Sunyaev-Zeldovich effect (SZ, Sunyaev and Zeldovich 1972)—, and by gravitational interactions acting on them during their travel from the last-scattering surface to the observer —causing both redshift and lensing effects. They are expected to be sub-dominant, at least in relation to the  $C_\ell$ , up to  $\ell \approx 2500$ .

The main physical effects producing the primary anisotropies and observed in the synchronous-comoving gauge (the observer's gauge) can be summarized in the following equation (Martínez-González, Sanz and Silk 1990, Sanz 1997):

$$\frac{\Delta T}{T}(\vec{n}) \approx \frac{\phi_e(\vec{n})}{3} + \int_e^o \frac{\partial \phi}{\partial t} dt + \vec{n} \cdot (\vec{v}_o - \vec{v}_e) + \left( \frac{\Delta T}{T}(\vec{n}) \right)_e \quad (5)$$

The first two terms in the r.h.s. account for the gravitational redshift suffered by the CMB photons in their travel toward us along the direction  $\vec{n}$ . They are called the Sachs-Wolfe (SW) and Integrated Sachs-Wolfe (ISW) effects, respectively (Sachs and Wolfe 1967). The third term is a Doppler effect due to the motion of the emitters at the last-scattering surface. Finally the fourth term is the temperature fluctuation at that surface.

Since the gravitational field has a large scale of interaction the SW and ISW effects dominate the angular power spectrum at the largest angular scales ( $\ell$  smaller than a few tens) producing an approximate plateau (see figure 2). Notice also that these scales are the most affected by the cosmic variance (see equation 4). The ISW effect has two contributions: an early one before recom-



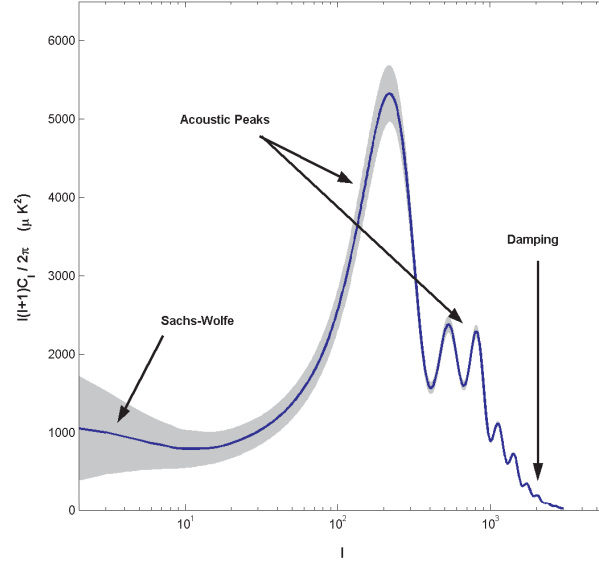


Figure 2.  $C_\ell$  for the best fit model given in Bennett et al. (2003) (see also table 2). The range of  $\ell$  where the different physical effects dominate is indicated. The gray band enveloping the  $C_\ell$  is the unavoidable error due to the cosmic variance (see text). The spectrum has been computed using the CMBFAST code (Seljak and Zaldarriaga 1996).

bination produced by the imperfect coupling of photons and baryons causing variations in the gravitational potential with time, and a late one after recombination due to changes in the gravitational potential with time. The late ISW effect is produced by the linear evolution of the large-scale matter distribution at later times if the universe is different from Einstein-de Sitter. As we will see at the end of Section 5 this is an independent test from the standard one (involving usually CMB, SN Ia or LSS data sets) about the existence of a dark energy component dominating the dynamics of the universe at recent cosmic times.

The Doppler effect plus the temperature fluctuations at the last-scattering surface dominate the shape of the angular power spectrum at  $\ell$  larger than a few tens. At multipoles above a hundred, the angular power spectrum exhibits a sequence of oscillations called acoustic peaks. They are driven by the balance between the gravitational force pulling to compress over-dense regions and radiation pressure pushing in the opposite direction. The position and amplitude of these oscillations are very much determined by the total energy content of the universe (or equivalently its geometry) and the nature and amount of the different components.

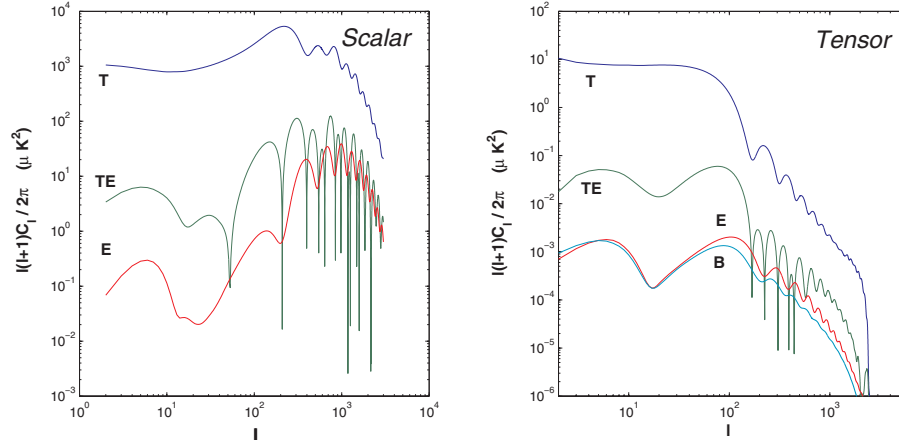


Figure 3. Temperature and polarization angular power spectra for scalar and tensor perturbations. The ratio tensor/scalar has been chosen to be  $r = 0.01$ . Apart from this parameter, the values for the rest of the parameters have been fixed to the values of the best fit model given in Bennett et al. 2003 (see also table 2). All the spectra have been computed using the CMBFAST code.

Finally, at large  $\ell$  ( $\gtrsim 1000$ ) the  $C_\ell$  power starts to decrease due to the width of the last-scattering surface and the imperfections of the coupling of the photon-baryon fluid (Silk effect, Silk 1968).

In Figure 2 one can see the range of  $\ell$  where the different effects dominate the angular power spectrum.

### 3. Polarization

Thomson scattering of the radiation generates linear polarization at the end of recombination when the growth of the mean free path of the photons allow anisotropies to grow (for a detailed description of the physics of polarization see, e.g., Challinor 2005). The expected level of polarization is only of  $\approx 5\%$ . From the Stokes parameters  $Q, U$  two rotationally invariant quantities can be constructed  $E, B$  (often referred to as the E-mode and B-mode, see Zaldarriaga and Seljak 1997, Kamionkowski et al. 1997). Under parity transformations  $E$  remains unchanged and  $B$  changes sign, and therefore the cross-power  $\langle a_{\ell m}^B a_{\ell m}^{T*} \rangle = \langle a_{\ell m}^E a_{\ell m}^{B*} \rangle = 0$ . It is for these parity properties that only three angular power spectra are required to characterise CMB polarization:  $C_\ell^E, C_\ell^B, C_\ell^{TE}$ .

An important property of the E,B decomposition is that whereas the E-mode polarization can be generated by both density perturbations and gravitational waves the B-mode can only be generated by the second ones. Therefore the detection of B-mode polarization is a unique proof of the existence of primordial

gravitational waves, opening the door to new areas of physics. In particular, it can also be used to impose strong constraints on the energy scale of inflation and on the shape of the inflaton potential. A complication comes from the lensing effect due to the gravitational potential of the LSS which converts part of the E-mode polarization in B-mode. Fortunately, this effect dominates over the primary one only at  $\ell \gtrsim 100$  leaving the rest of the spectrum unaltered. All the temperature and polarization angular power spectra for scalar and tensor perturbations are plotted in figure 3.

As for the temperature angular power spectrum, the accuracy in the determination of the polarization angular power spectra has also a fundamental limit imposed by the cosmic variance. For Gaussian distributed anisotropies the errors in  $C_\ell^E, C_\ell^B, C_\ell^{TE}$  are given by:

$$\Delta C_\ell^{E,B} = \frac{1}{\sqrt{\ell + 0.5}} C_\ell^{E,B}, \quad \Delta C_\ell^{TE} = \frac{1}{\sqrt{\ell + 0.5}} \left( C_\ell^T C_\ell^E + C_\ell^{TE2} \right)^{1/2}. \quad (6)$$

There are a number of Galactic and extragalactic foregrounds which complicate the observation of the CMB polarization. Although their relevance depends very much on the frequency they are expected to be very harmful, specially for the B-mode due to its relatively small amplitude. For a recent estimate of the effect of foregrounds on the polarization observations see Tucci et al. (2005).

Only recently the DASI experiment has been able, for the first time, to detect anisotropies in polarization (Kovac et al. 2002). Afterward, the WMAP experiment measured the TE angular cross-power spectrum with more precision and covering a much wider range of scales (Kogut et al. 2003). More recently the CBI experiment has measured the E angular power spectrum with more resolution than DASI allowing the detection of the second, third and fourth acoustic peaks (Redhead et al. 2004b).

In addition to the temperature anisotropies, the anisotropies in polarization contain very relevant and independent information. In particular, in the standard model the maxima in the E spectrum are out of phase with those in the T spectrum due to the fact that polarized radiation is sensitive to the velocity of the fluid, and the velocity and density are out of phase in an acoustic wave. This shift is precisely what has been recently reported by Redhead et al. (2004b) based on CBI data (see figure 7 below). As we will see later, anisotropies in the polarization are very relevant to confirm the best fit model given by the temperature data and to constrain specific parameters as the optical depth to which they are very sensitive.

#### 4. Cosmological parameters

There are a number of cosmological parameters that account for very different fundamental physical properties of the universe and that influence the

radiation angular power spectrum in many ways. These parameters characterize the background model of the universe (assumed to be the homogeneous and isotropic Friedmann-Robertson-Walker model), the primordial scalar and tensor fluctuations and the reionisation history. At present around 12 parameters are considered for the data analysis.

The parameters characterizing the background model of the universe are the following:

- *Physical baryonic density,  $w_b$ :  $w_b = \Omega_b h^2$ .*
- *Physical matter density,  $w_m$ :  $w_m = \Omega_m h^2$ .  $\Omega_m$  is given by the sum of the baryonic density  $\Omega_b$ , the CDM density  $\Omega_{CDM}$  and the neutrino density  $\Omega_\nu$ .*
- *Physical neutrino density,  $w_\nu$ :  $w_\nu = \Omega_\nu h^2$  (up to now only upper limits are found for this parameter).*
- *Dark energy equation of state parameter,  $w$ :  $w \equiv p_{DE}/\rho_{DE}$ .*
- *Dark energy density,  $\Omega_{DE}$ : In case  $w$  were constant and took the value  $-1$  then the dark energy takes the form of a cosmological constant and its energy contribution is represented by  $\Omega_\Lambda$ .*
- *Hubble constant,  $h$ :  $h \equiv H_0/100 \text{ km s}^{-1} \text{ Mpc}^{-1}$ .*

The reionisation history of the universe influences the CMB by a single parameter:

- *Optical depth,  $\tau$ :  $\tau = \sigma_T \int_{t_r}^{t_0} n_e(t) dt$ , where  $\sigma_T$  is the Thomson cross-section and  $n_e(t)$  is the electron number density as a function of time.*

The cosmological parameters that characterize the matter and gravitational waves primordial power spectra are:

- *Amplitude of the primordial scalar power spectrum,  $A_s$ :  $P_s(k) = A_s (k/k_0)^{n_s}$ , where  $k_0 = 0.05 \text{ Mpc}^{-1}$ .*
- *Scalar spectral index,  $n_s$ .*
- *Running index,  $\alpha$ :  $\alpha = dn_s/d \ln k$ . It accounts for the deviations from a pure power-law. Its value is normally determined at the scale  $k_0 = 0.05 \text{ Mpc}^{-1}$ .*
- *Tensor-to-scalar ratio,  $r$ :  $r = A_t/A_s$ .*
- *Tensor spectral index,  $n_t$ : from the consistency relation of inflation it is normally assumed that  $n_t = -r/8$ .*

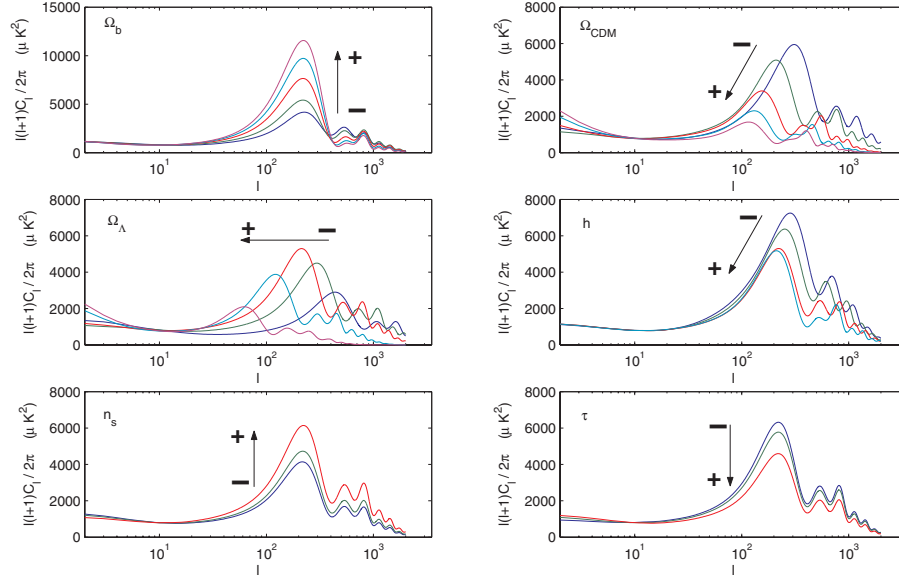


Figure 4. Dependence of  $C_\ell$  on some relevant cosmological parameters (The  $C_\ell$  has been produced with the CMBFAST code).

Besides those parameters there are two possible types of primordial matter density fluctuations: adiabatic (the entropy per particle is preserved) and isocurvature (matter fluctuations compensate those of the radiation conserving total energy density). As commented in the Introduction the standard model of inflation predicts fluctuations of the adiabatic type.

Analyses that combine CMB with LSS require an additional parameter accounting for the bias  $b$  of the galaxy density respect to the matter density.

In figure 4 we show the changes in  $C_\ell$  produced by the variation of some of the most relevant cosmological parameters. The many different ways in which the  $C_\ell$  can vary with the parameters produces degeneracies complicating their accurate determination. In particular, there is a well known geometric degeneracy involving the matter and dark energy densities. This is shown in figure 5 where almost identical angular power spectra are obtained for three different values of the curvature ( $\Omega_k = 1 - \Omega_m - \Omega_{DE}$ ). This example illustrates the need of including in the analysis additional cosmological data sets (like SN Ia, LSS, cluster density, CMB polarization, ...) to break the degeneracies.

## 5. Cosmological constraints

In recent years there has been an explosion of cosmological data which have made possible a strong advance in the determination of the cosmological para-

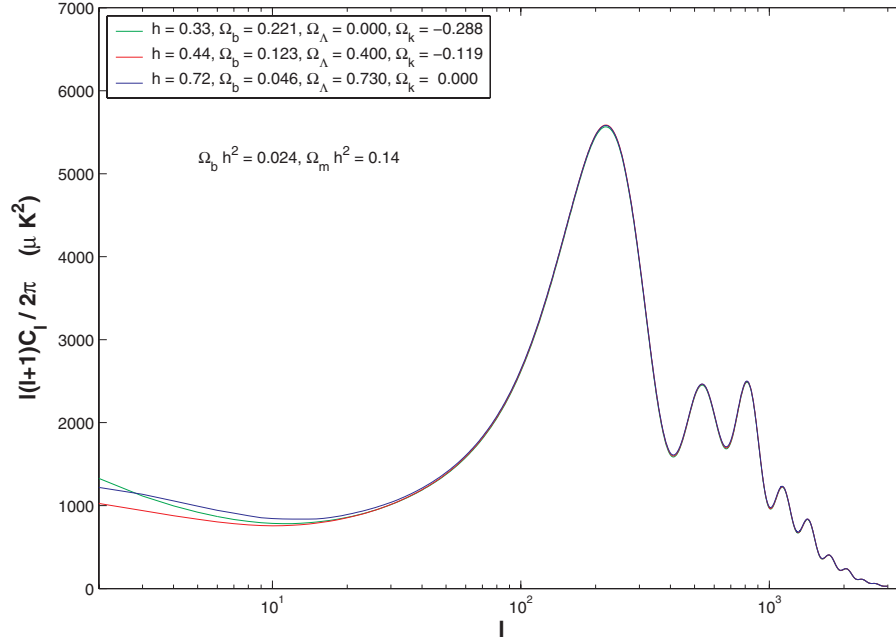


Figure 5. Geometric degeneracy for three values of the curvature  $\Omega_k$ . Apart from the parameters given in the figure the rest of the parameters have been fixed to the best fit model given in Bennett et al. (2003). The three spectra have been computed using the CMBFAST code.

meters. Below we summarize the main results for CMB data alone and when combined with other cosmological data sets.

### WMAP and higher resolution CMB experiments

The WMAP data alone is able to put strong constraints on some cosmological parameters when some priors are assumed in the analysis (Spergel et al. 2003). Table 1 summarizes the results when a flat universe is assumed, the prior  $\tau < 0.3$  is imposed on the optical depth and only 6 parameters are considered. It is interesting to notice that the Einstein-de Sitter universe (i.e. a spatially flat universe with null dark energy) is rejected at a very high confidence level. Besides, the value of the optical depth parameter  $\tau$  is essentially determined by the TE angular cross-power spectrum.

The WMAP data also test the type of the primordial fluctuations. The clear detection of the first acoustic peaks as well as the detection of the TE cross-correlation imply that the fluctuations were primarily adiabatic, in agreement with the standard inflationary model.

Table 1. Cosmological parameters using only WMAP data. In the fit the universe is assumed to be spatially flat and the value of the optical depth is constrained to  $\tau < 0.3$  (from Spergel et al. 2003)

Parameter	Values (68% CL)
$w_b$	$0.024 \pm 0.001$
$w_m$	$0.14 \pm 0.02$
$h$	$0.72 \pm 0.05$
$A_s$	$0.9 \pm 0.1$
$\tau$	$0.166^{+0.076}_{-0.071}$
$n_s$	$0.99 \pm 0.04$

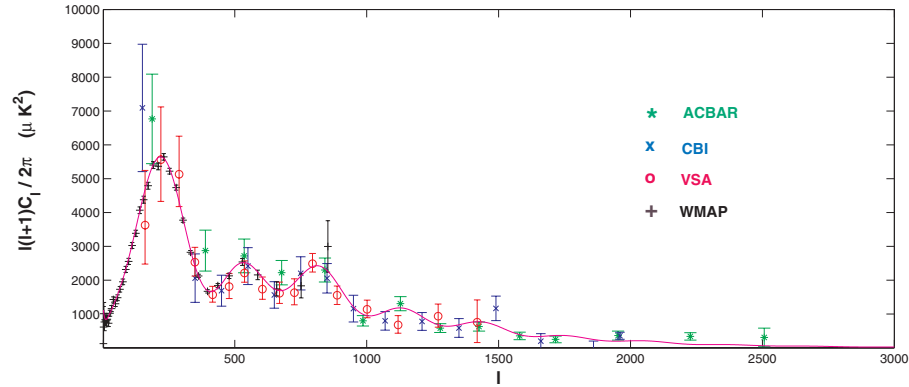


Figure 6.  $C_\ell$  measured by WMAP, ACBAR, CBI and VSA, together with the best fit model given by Bennett et al. (2003). The values of the parameters are listed in table 2.

The situation is improved if temperature data from high resolution CMB experiments is included in the analysis (Spergel et al. 2003, Dickinson et al. 2004). In figure 6 the  $C_\ell$  obtained from the experiments WMAP (Hinshaw et al. 2003), ACBAR (Kuo et al. 2004), CBI (Readhead et al. 2004a) and VSA (Dickinson et al. 2004) is shown. Although the polarization measurements are not yet sensitive enough to significantly improve the constraints already derived from the temperature one (except for  $\tau$ ), however the measured peaks in the E-mode  $C_\ell$ , which are out of phase with the temperature  $C_\ell$  ones, suppose an independent evidence of the standard model and, more specifically of the adiabatic type of the primordial matter density fluctuations. The TE angular cross-power spectrum from DASI (Leitch et al. 2004), WMAP (Kogut et al. 2003) and CBI (Readhead et al. 2004b) as well as the E-mode polarization angular power spectrum from DASI and CBI are shown in figure 7.

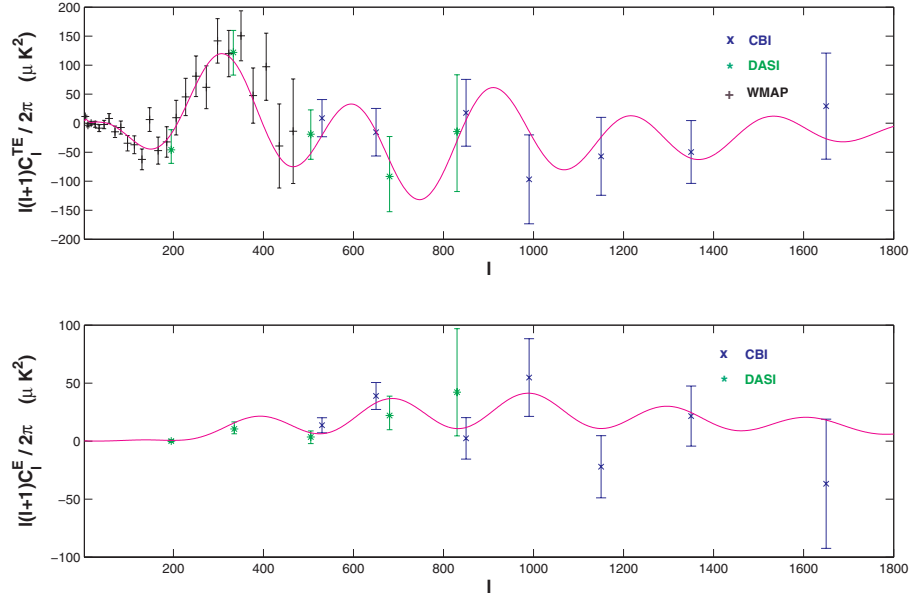


Figure 7. TE and E angular power spectra measured by DASI, WMAP and CBI (TE) and DASI and CBI (E). Also plotted is the best fit model given by Bennett et al. (2003). The values of the parameters are listed in 2.

## Combination with other cosmological data sets

The present richness of data is not exclusive of the CMB. Also large galaxy surveys covering a large fraction of the sky and measuring the three-dimensional power spectrum using  $\approx 200000$  redshifts, like the 2dFGRS (Percival et al. 2001) or SDSS (Tegmark et al. 2004a), have been recently achieved. If the initial fluctuations are Gaussian, all the information is included in the power spectrum  $P(k)$  and thus this is the quantity normally used for the analysis. The cosmological parameters determine the matter power spectrum at present through the initial amplitude and the spectral index  $A_s, n_s$  and the transfer function connecting linearly the present and initial  $P(k)$ . An additional bias parameter  $b$ , assumed to be scale-independent and linear, is needed to relate galaxy and matter density. Moreover, non-linear evolution of the matter density power spectrum should be also considered in the comparison with observations. The present matter density power spectrum as well as the luminosity distance-redshift diagram determined with SN Ia depend on the cosmological parameters in a very different way from the  $C_\ell$ , and so the combined data sets can potentially impose much more severe constraints. Results of combining CMB data with LSS galaxy surveys (Percival et al. 2001, Tegmark et al. 2004a), HST key project value of  $H_0$  (Freedman et al. 2001), SN Ia



magnitude-redshift data (Riess et al. 2001, Tonry et al. 2003), Ly $\alpha$  forest power spectrum (Croft et al. 2002, McDonald et al. 2004) are given in Bennett et al. (2003), Spergel et al. 2003, Tegmark et al. (2004b) and Seljak et al. (2004). As it is shown in these papers, the constraints on the cosmological parameters are greatly improved when combining all those cosmological data sets and, what is even more important, the best fit model is an acceptable fit for all of them. Table 2 shows the best fit cosmological parameters given in Bennett et al. (2003) for the combination WMAP+CBI+ACBAR+2dFGRS. Alternative combinations include WMAP, high redshift SN Ia and abundances of rich clusters of galaxies (see e.g. Rapetti, Steven and Weller 2005 and Jassal, Bagla and Padmanabhan 2005 for a detailed analysis of the constraints imposed by these data sets on the dark energy equation of state). In figure 8 confidence contours are given for the  $(\Omega_m, \Omega_{DE})$  plane combining WMAP, SN Ia (Knop et al. 2003) and galaxy cluster abundance (Allen et al. 2002). The complementarity of the three data sets is clearly noticed by the reduction of the contours of the combined data set compared to the individual ones.

Table 2. Cosmological parameters from WMAP, CBI, ACBAR and 2dFGRS combined data (from Bennett et al. 2003)

Parameter	Values (68% CL)
$w_b$	$0.0224 \pm 0.0009$
$w_m$	$0.135^{+0.008}_{-0.009}$
$w_\nu$	$<0.0076$ (95% CL)
$w$	$<-0.78$ (95% CL)
$\Omega_{DE}$	$0.73 \pm 0.04$
$h$	$0.71^{+0.04}_{-0.03}$
$\tau$	$0.17 \pm 0.04$
$A_s$	$0.833^{+0.086}_{-0.083}$
$n_s$	$0.93 \pm 0.03$
$\alpha$	$-0.031^{+0.016}_{-0.018}$
$r$	$<0.90$ (95% CL)

## Integrated Sachs-Wolfe effect

There are strong evidences that the universe today is dominated by the dark energy density  $\Omega_{DE}$ . The evidences came first from measurements of the luminosity curve and redshift of distance SN Ia, and later from surveys of the CMB anisotropy and LSS distribution of galaxies. More recently there have been independent tests that confirm this result. They come from the cross-correlation of the CMB map with LSS surveys which span a wide range in redshift. From the late ISW effect a non null signal is expected due to the fact

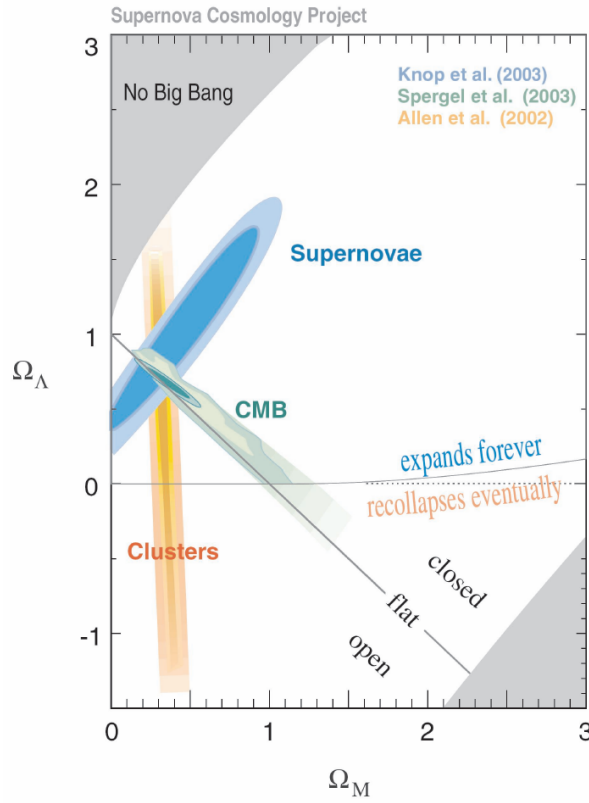


Figure 8. Confidence contours for the plane  $(\Omega_m, \Omega_\Lambda)$  using SN Ia, CMB and cluster density data (taken from the Supernova Cosmology Project).

that the same gravitational potential created by the LSS at late times is also leaving an imprint on the CMB anisotropies. The amplitude and sign of the effect are determined by  $\Omega_{DE}$ ,  $\Omega_k$  and  $h$ . If the universe is close to spatially flat, as found in a consistent way by very different cosmological data sets, then a positive LSS-CMB cross-correlation would be an unambiguous indication of the presence of dark energy.

This is what has been recently found by a number of authors using different surveys and methods (Boughn and Crittenden 2004; Fosalba, Gaztañaga and Castander 2004; Nolta et al. 2004; Afshordi, Loh and Strauss 2004; Vielva, Martínez-González and Tucci 2004). The maximum amplitude for the signal has been obtained in the latter paper by cross-correlating the radio galaxy sur-